Formulation of silymarin surface modified vesicles: In vitro characterization to cell viability assessment

Syed Sarim Imam, Sultan Owaid Alshammari, Sultan Alshehri [*], Wael A. Mahdi, Mohamed H. Al-Agamy

Department of Pharmaceutics, College of Pharmacy, King Saud University, Riyadh 11451, Saudi Arabia

ABSTRACT

Silymarin (SLR) is a poorly water-soluble bioactive compound with a wide range of therapeutic activities. Nanosized silymarin vesicles (F1–F6) were prepared by the solvent evaporation rehydration method. The silymarin vesicles were evaluated for vesicle size, surface charge, entrapment efficiency, and drug release studies. The optimized SLR lipid vesicle (F3) was further modified with the addition of the cationic polymer chitosan. After that, the modified vesicle (F3C1) was assessed for permeation flux, antimicrobial activity, cell viability, and molecular docking studies. The silymarin vesicles showed nanometric size (<250 nm), low polydispersibility index (<0.05), negative surface charge, and high SLR entrapment (85–95 %). The drug release study result demonstrated a maximum drug release of 91.2 ± 2.8 %. After adding chitosan to the surface, there was a significant change in the size, polydispersibility index, surface charge (positive), and encapsulation efficiency. The drug release was found to be prolonged, and the permeation flux was also increased in comparison to free SLR. A comparative antimicrobial result was observed in comparison to the free SLR and standard drug. The cell viability assay also demonstrated a low IC_{50} value for F3C1 against the cell line.

1. Introduction

Lipid vesicles are nanoscale colloidal system having a hydrophilic inner cavity and a lipid bilayer (Haddad et al., 2023). Phospholipids or synthetic amphiphiles are the structural components of vesicles; they can be mixed with sterols to improve the membrane's permeability (Bulbake et al., 2017). It is a biocompatible delivery system and can encapsulate both the water soluble and insoluble drugs. It can modulate the drug release and protect the drug from the rapid degradation (Melchior et al., 2023; Moya-Garcia et al., 2023). The beneficial effects of natural bioactive compound may be limited by their poor bioavailability and stability (Asmaa et al., 2023; De Luca et al., 2022). The lipid vesicles can be successfully developed to improve the bioavailability, stability, prevents the degradation, and retain their antioxidant action (Guimaraes et al., 2021). This delivery strategy has drawn increased attention because it can accelerate the intracellular transport and extend the retention of entrapped antioxidants inside the cell (Machado et al., 2019; Suntres, 2011).

Bioadhesive polymers can also be used to modify the surface of vesicles in order to enhance the drug entrapment, physical and colloidal stability, and bioavailability (Sun et al., 2020; Megahed et al., 2022; Zhang et al., 2019). Since non-adhesive nano-carrier uptake is hampered by high interstitial intratumoral pressures (Moya-Garcia et al., 2023). **So,** chitosan (CHT) can be used as a mucoadhesive agent by altering the anionic vesicles' surface. It aids in keeping the medication within the vesicle and improves drug absorption at the tumor's target location (Sun et al., 2020; Alomrani et al., 2019; Dawoud, 2021; Pandey et al., 2022). It binds to the anionic glycoproteins in mucin by electrostatic interactions (Collado-González et al., 2019). Additionally, it has been demonstrated that chitosan-coated nanocarriers enhances transcellular and paracellular drug transport and have a decreased aggregation in the liver and blood (Moya-Garcia et al., 2023; Megahed et al., 2022; Pandey et al., 2022). There are numerous chitosan coated drug delivery systems developed and reported for their biological activities (Hilitanu et al., 2024; Sharifi-Rad et al., 2021; Confederat, et al., 2021).

Silymarin (SLR: Fig. 1) is a blend of various flavonolignans (flavonoids) that are extracted from the fruits of Silybum marianum (L.) Gaertn. (asteraceae) (Chambers et al., 2017; Piazzini et al., 2019). Its
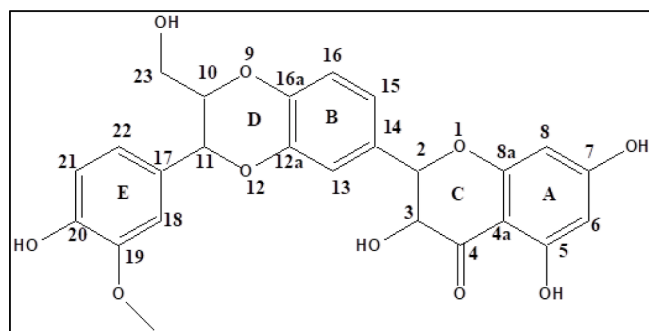

Fig. 1. Chemical Structure of Silymarin.

innate antiviral, antioxidant, anti-inflammatory, and antifibrotic properties have led to its usage as a therapeutic agent, including hepatocellular carcinoma (Federico et al., 2017). Additionally, it has proven to have antimetastatic and chemo preventive effects in a variety of malignancies (Fallah et al., 2021; Venugopal et al., 2023). Its weak permeability through the gut's epithelial cells, quick clearance, poor water solubility and low bioavailability (Clichici et al., 2020). Even after continuous dosing, it has shown a high safety profile without toxicity (Koltai and Fliegel, 2022).

The different SLR formulations have been developed that increase SLR bioavailability in order to navigate the above problems. Enhancing SLR bioavailability and therapeutic efficacy could be greatly aided by the application of different delivery systems (Ma et al., 2017). In order to address these shortcomings, specifically the low water solubility restricted its oral bioavailability. A number of approaches like nanoparticles (Younis et al., 2016; Piazzini et al., 2018; Liang et al., 2018; Abdullah et al., 2022), liposomes (Kumar et al., 2014; Yang et al., 2015), micro-/nanoemulsions (Piazzini et al., 2017), and polymeric micelles (Piazzini et al., 2019; El-Far et al., 2016; Soodvilai et al., 2019) have been reported.

Therefore, the present study's objective was to prepare and evaluate the SLR vesicles and surface-modified SLR vesicles. For SLR vesicles, chitosan is employed as a surface-modifying polymer. To the best of our knowledge, no reports exist where SLR vesicles were combined with surface-modifying polymers. The physicochemical characteristics of the vesicles (F1 – F6) and surface modified vesicles (F3C1, F3C2) included mean vesicle size, surface charge, encapsulation efficiency, and drug release. Additionally, the antibacterial, antioxidant, and cell viability studies of SLR vesicles and surface-modified vesicles were compared with free SLR.

2. Materials

Silymarin, methanol, chloroform, Mueller Hinton (MH) Agar, Tryptic Soy Agar (TSA) were procured from Sigma Aldrich, ST Louis MO, USA. Chitosan was purchased from ACROS ORGANICS, New Jersy, USA. Lipid was received as a gift sample from LIPOID, GMBHFRIGEN-STRASSE 4, LUDWIGSHAFEN. Cholesterol and Tween 80 was used in this study purchased from ALPHA CHEMIKA, INDIA and Eurostar Scientific Ltd Liverpool, UK. Sensi – Discs purchased from Becton, Dickinson and Company, MD21152 USA. American type cell culture cell line HepG2 was used. All the other chemicals and solvents used were of AR grade.

2.1. Formulation of SLR vesicles and surface modified vesicles

SLR loaded vesicles were prepared by the solvent evaporation technique using the lipid, cholesterol and surfactant (Parsa et al., 2023). The composition of the SLR lipid vesicles shown in Table 1. Calculated amount of SLR was taken and dissolved in the minimum volume methanol and sonicated for complete solubilization. Separately, lipid

Table 1
Formulation composition and their characterization results.

Code	Lipid	CHL: PC (molar ratio)	CHT (%)	VS(nm)	PDI	SC(mV)	EE(%)
F1	250	1:2		191.4 ± 5.3^{ns}	0.28	$-13.2 \pm 1.1^{**}$	81.4 ± 2.7
F2	250	1:3		201.1 ± 2.7^{ns}	0.39	$-15.1 \pm 1.1^{*}$	86.3 ± 1.9
F3	250	1:4		198.6 ± 4.3	0.38	-19.6 ± 2.4	91.2 ± 2.5
F4	250	4:1		$237.2 \pm 2.9^{**}$	0.31	-21.7 ± 2.2^{ns}	88.1 ± 2.3
F5	250	3:1		$228.8 \pm 5.9^{**}$	0.32	-18.1 ± 1.4^{ns}	87.4 ± 3.1
F6	250	2:1		207.1 ± 4.1^{ns}	0.57	-17.2 ± 1.1^{ns}	83.1 ± 3.3
F3C1	250	1:4	0.25	219.2 ± 4.7	0.34	$+21.6 \pm 1.8$	82.1 ± 2.4
F3C2	250	1:4	0.50	$261.5 \pm 1.6^{**}$	0.41	$+28.5 \pm 1.5^{**}$	77.6 ± 1.9

EE: entrapment efficiency; CHL: cholesterol; PC: phosphatidylcholine; SC: surface charge; PDI: polydispersibility index; CHT: chitosan; VS: vesicle size. Statistical analysis was performed by comparing F3 with F1, F2, F4, F5, F6 and F3C1 with F3C2. Dunnett Multiple Comparisons test was performed and p value < 0.0001 considered significant.

and cholesterol was dissolved in the chloroform methanol mixture. Both the solution mixed together in a round bottom flask and fitted to the rotary evaporator. The organic solution was evaporated at reduced pressure with rotation speed of 100 rpm. A thin film is formed on the wall of round bottom flask and then kept in an airtight desiccator to remove the residue of organic solvent for 48 h. After that the lipid film was rehydrated with PBS in a rotary evaporator for 2 h to complete swelling of vesicles. The silymarin vesicles were collected in the glass vials and kept at room temperature for stability. It was probed in ice condition for the reduction of size and then characterized for different parameters (Asmaa et al., 2023). The optimized SLR lipid vesicle (F3) was further coated with chitosan (0.25 and 0.50 %). The sample F3 was taken and mixed with equal volume of filtered CHT solution prepared in acetic acid. Both mixtures were kept on the magnetic stirrer for 24 h with continuous stirring. Finally, the chitosan silymarin vesicles (F3C1 and F3C2) were collected and characterized for vesicle size, polydispersibility index, surface charge and encapsulation efficiency (Ang et al., 2023).

2.2. Characterization

2.2.1. Vesicle size and charge

The vesicles were evaluated for mean size, polydispersibility index (PDI) and surface charge (ZP). The silymarin vesicles (F1-F6, F3C1, F3C2) were diluted (100-folds) and transferred to cuvette for measurement (Malvern zeta sizer; UK). The same samples were transferred to different cuvette to measure the surface charge. The study was performed in triplicate and data shown as mean ± SD.

2.3. Entrapment efficiency

The amount of SLR entrapped inside the vesicles were measured by the ultracentrifugation method (Maryam et al., 2023). The samples were taken in the tube and centrifuged at 10,000 rpm (Centurian Scientific, Germany) at 4 °C for 60 min. The supernatants were collected and diluted with methanol to measure the SLR content in each formulation by the UV spectrophotometer at 288 nm (El-Samaligy et al., 2006). The calibration was plotted between the concentration of 10 – 80 µg/mL to calculate the amount of drug present in the supernatant and then the amount of entrapped drug was measured using the below formula (Hilitanu et al., 2024):

$$EE\,(\%) \,=\, \left[\frac{Wa - Wb}{Wa}\right] x100$$

Wa = Initial amount of SLR added; Wb = Amount of SLR unentrapped in vesicles.

2.4. Drug release

This study was performed for SLR lipid vesicles (F1-F6, F3C1, F3C2) to check the release pattern. The release data was compared with each other to assess the change in release pattern in each composition. Each sample (containing 5 mg of SLR) was taken and filled to the dialysis bag (Micheli et al., 2023). The sample filled bag tied from both ends and dipped into the release media (500 mL). The release media temperature was set at 37 °C and rotated at 100 rpm. At each time point, the released content (3 mL) was collected and replaced with the same volume of fresh blank media. The collected released samples were filtered and the amount of SLR measured using spectrophotometer.

2.5. Differential scanning calorimetry

The calorimetry study was performed to check the drug crystallinity after encapsulation into the lipid vesicle (F3, F3C1). The thermogram of each sample (free SLR, lipid, CHL, chitosan and SLR lipid vesicles (F3, F3C1) was taken into an aluminium pan to compare the melting behavior. The study was performed by the DSC thermogram (Perkin Elmar, Shelton, USA). The study was performed between the temperature range of 30–250 °C with heating speed of 10 °C. A continuous supply of nitrogen is given throughout the study and a blank pan is kept as reference.

2.6. Infra-red spectroscopy

The spectroscopy study was performed to check the drug polymer interaction study (Singh et al., 2022). Each sample (free SLR, lipid, cholesterol, chitosan and SLR lipid vesicles (F3, F3C1). The study was performed by the ATR technique (Bruker ATR, Germany). The spectra of each pure sample were compared with the formulations (F3, F3C1) to check the change in peak position and peak intensity.

2.7. Permeation study

The amount of SLR permeated across the artificial membrane was performed by the Franz diffusion cell. The diffusion cell assembly (effective surface area 1.2 cm^2, volume 22 ml) was fixed and the study was performed at a temperature of 37 °C with 100 rpm. The sample of optimized SLR formulations (F3, F3C1) and their permeation and flux value was calculated and compared with the free SLR. Each sample was filled to the donor chamber and at a fixed time point (1 h, 2 h, 3 h, 4 h, 5 h, 6 h) the permeated amount of content collected and at the same time refilled with fresh blank media. The collected samples were filtered and the amount of SLR permeated was measured using UV spectrophotometer. The absorbance was used to calculate the drug permeation across the membrane.

2.8. Antimicrobial study

The antibacterial activity was performed for the samples (free SLR, and F3C1) using the cup diffusion agar method. This method was done according to the guidelines of CLSI (CLSI, 2022). The samples were tested for the antibacterial activity against six standard bacterial strains. Four gram positive bacterial strains (*Staphylococcus aureus* ATCC 25923, *Micrococcus luteus* ATCC 10240, *Bacillus subtilis* ATCC 10400, and *B. pumilus* ATCC 7743) and two gram negative rods (*Escherichia coli* ATCC 25922 and *Pseudomonas aeruginosa* ATCC 27853). The bacterial strains were inoculated onto the TSA plate medium. The inoculated

plates were incubated at 37 °C for 20 h in ambient condition. Three to five pure colonies of overnight culture were taken by the aid of the inoculating loop, then the loopful was suspended in three mL of sterile 0.9 % sodium chloride. The suspension was mixed carefully by the aid of the vortex mixer. The suspension was matched with the turbidity of 0.5 McFarland reagent. The matched bacterial suspension was diluted according to the CLSI guidelines with a final stock suspension of 1×10^6 colony forming unit (CFU)/mL. The sterile cotton swab was dipped in the adjusted bacterial suspension and the swab was turned against the side of the tube to remove the excess inoculum. The suspension was swabbed evenly over the surface of the MHA plate. Two cups were made in the inoculated MHA plate by aid of the cork borer. Aliquot (200 μL) of each sample was added into the cup by the aid of automatic pipette. Imipenem (10 μg) disc was used as antibacterial quality standard control while DMSO was used as negative control. The plates were incubated aerobically at 37 °C for 20 h. After the incubation time, the results were recorded manually by determining the zone of inhibition (mm) by aid of the measuring ruler. The experiment was carried out in duplicate and the mean value was calculated.

2.9. Antioxidant assay

The assay of the free SLR and optimized silymarin surface modified vesicles (F3C1) was performed by the DPPH and ABTS methods. Both the samples were prepared separately in a concentration range of 5–100 μg/mL in the solvent. Each concentration of sample was added to the DPPH solution and kept aside in dark for the complete reaction mixture. After that each sample absorbance was measured at 517 nm using a spectrophotometer. In case of ABTS assay, the test samples (free SLR and F3C1) were added to ABTS solution and allowed to be kept aside for 6 h to complete the reaction to produce the ABTS radicals during this time. Finally, the sample absorbance was measured at 734 nm.

2.10. Cell line study

The cell line study of the silymarin vesicles F3, F3C1 and free SLR was tested against the HepG2 cancer cell lines. The cancer cells were cultured in the DMEM media with fetal bovine serum. Penicillin-streptomycin (1 %) was added to the medium and continuous supply of CO$_2$ (5 %) was supplied for growth of cancer cells. The cancer cells (1 $\times$ 10^5 cells/well) were cultured in the 96 well plate and kept in an incubator for 24 h for complete growth. Each test sample (free SLR, F3, F3C1) was added to the well in different concentrations (10–500 μg/mL) and their results were compared at 24 h. The treated 96 well plate was kept in an incubator overnight and then MTT solution (20 μL) dye was added to each well and incubated for 4 h. After that the medium was discarded and DMSO (100 μL) was replaced and again incubated for 30 min in dark (Keshavarz et al., 2023). The absorbance of each well was measured at 570 nm using a microplate reader. IC$_{50}$ of each sample was calculated by fitting the results to a Graph Pad Prism software (Gutierrez-Saucedo et al., 2023).

2.11. Molecular docking

The computational analysis was performed to exhibit the feasible interactions between the drug Silymarin, cholesterol, chitosan and lipid against human hepatocellular carcinoma (HepG2) cells. VEGFR-2 plays a significant role in solid tumors. Several reports have already established the relationship between VEGFR-2 expression and hepatocellular carcinoma (Huang et al., 2011). Therefore, to accomplish docking study of drug & carriers (considered as ligands) against the vascular endothelial growth factor receptor-2 (VEGFR-2), the target site having PDB ID: 3V2A was downloaded from RCSB PDB database (http://www.rcsb.org). As per the prior studies (El-Shehawy et al., 2023) chain A was selected. For the refinement and preparation process, the energy was minimized for the downloaded macromolecule by using the AutoDock

Tools version 1.5.6. (https://www.autodock.scrips.edu; La Jolla, CA, USA). The ligands (drug & carriers) smile notation was retrieved from the pubchem (https://pubchem.ncbi.nlm.nih.gov/). The smiles notation of the ligands was converted into PDBQT format [Protein Data Bank, Partial charge (Q) and Atom type (T)] with the help of OpenBabel GUI program. The default charges energy parameters were selected for both macromolecules and ligands. A grid box was prepared to trace the path. An auto grid was run to fetch the various docked conformation of the ligand with the receptor exhibiting minimum binding score.

2.12. Statistical analysis

Statistical analysis was performed using Graph Pad Prism (Version 8, San Diego CA, USA). The study performed in triplicate and data shown as mean $\pm$ SD. Dunnet Multiple Comparisons test was performed and p value < 0.0001 considered significant.

3. Results

3.1. Vesicle size and charge

The mean size, polydispersibility index (PDI) and surface charge (ZP) of SLR vesicles (F1-F6, F3C1, F3C2) were evaluated and shown in Table 1. The vesicle size of the formulation (F3 and F3C1) was found to be 198.6 nm and 219.2 nm, and selected as optimum formulation for further characterization (Fig. 2A-B). PDI is also an important factor which helps to identify the stability of the formulations. It ranges from 0 to 1, and the low PDI value leads to greater homogeneity. The optimized silymarin vesicles F3 and F3C1 depicted the PDI value of 0.38 and 0.34, respectively. The surface charge of the silymarin vesicles (F1 − F6) was found to be negatively charged (−13.2 to − 21.7 mV). The selected SLR lipid vesicles (F3) showed the maximum surface charge of – 19.6 mV. The surface modified SLR lipid vesicles (F3C1 and F3C2) displayed positive surface charge of 21.6 21.6 $\pm$ 1.8 and 28.5 $\pm$ 1.5 mV, respectively.

3.2. Entrapment efficiency

The change in the vesicle composition gives significant (p < 0.01) variation in the SLR entrapment as shown in Table 1. The lowest entrapment was found with the SLR lipid vesicle (F1) with 81.4 $\pm$ 2.7 % and maximum was shown by the vesicle (F3) with 91.2 $\pm$ 2.5 %. The optimized SLR lipid vesicles (F3) surface was modified and their entrapment was also calculated. The chitosan concentration also showed a greater impact on the EE. A significant (p < 0.01) reduction in the EE was observed after addition of chitosan. As the concentration of chitosan increases the EE % also decreases. SLR lipid vesicle (F3C1 prepared with 0.25 % CHT) showed 82.1 $\pm$ 2.4 % in comparison to F3 (91.2 $\pm$ 2.5 %). Further increase in CHT concentration from 0.25 to 0.50 %, EE % reduces and reaches 77.6 $\pm$ 1.9.
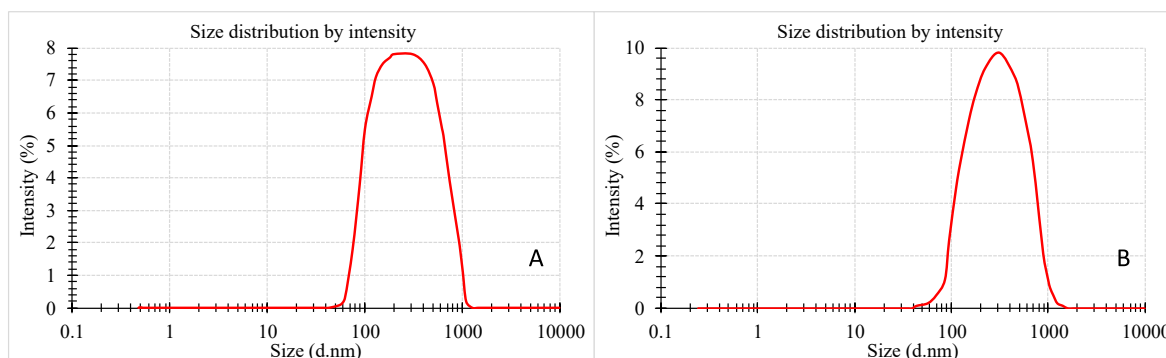
3.3. Drug release

The study was performed for SLR vesicles (F1-F6, F3C1, F3C2) and the data shown in Fig. 3. The variation in the vesicles composition leads to difference in the maximum drug release. The vesicles (F2) showed a significantly (p < 0.01) lower SLR release (83.1 $\pm$ 2.5 %). The other vesicles (F3, F4) showed a significantly (p < 0.01) higher SLR release than the formulation (F2). The maximum drug release displayed by the formulation F3 with 94.9 $\pm$ 2.1 % followed by 93.3 $\pm$ 2.4 % (F4). The release pattern was found as follows: F3 > F4 > F1 > F5 > F6 > F2. The other silymarin vesicles (F1, F5, F6) showed non-significant (ns) difference in the release pattern. The vesicle F3C1 and F3C2 showed the maximum SLR release of 72.1 $\pm$ 3.1and 60.8 $\pm$ 3.5 %. The addition of chitosan to the optimized SLR lipid vesicles (F3) displayed a significant (p < 0.001) change in the release pattern. As the concentration of chitosan increases, a significant (p < 0.01) reduction in the drug release was achieved.

3.4. Differential scanning calorimetry

The thermogram of free SLR, lipid, cholesterol and optimized SLR lipid vesicles (F3 and F3C1) was shown in Fig. 4. The free SLR displayed the endothermic peak at 142.4 °C. The other ingredients cholesterol and lipid showed the melting point of 137.9 °C, and 122.4 °C. In case of silymarin vesicles F3 and F3C1 the melting peak of SLR diminishes may be due to the solubilization in the used carrier.

3.5. Infra-red spectroscopy

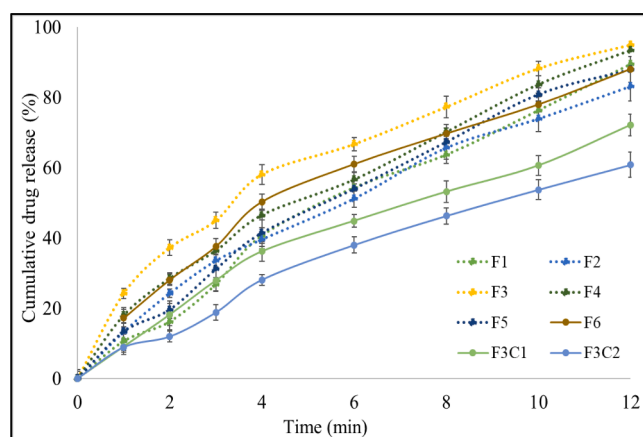The manifested frequency as shown in Fig. 5 for the free SLR,

Fig. 3. Release data of Silymarin vesicles (F1-F6) and Silymarin surface modified vesicles (F3C1, F3C2).

Fig. 2. A-B: Mean diameter of (A). Silymarin vesicles (F3) and (B). Silymarin surface modified vesicles (F3C1).
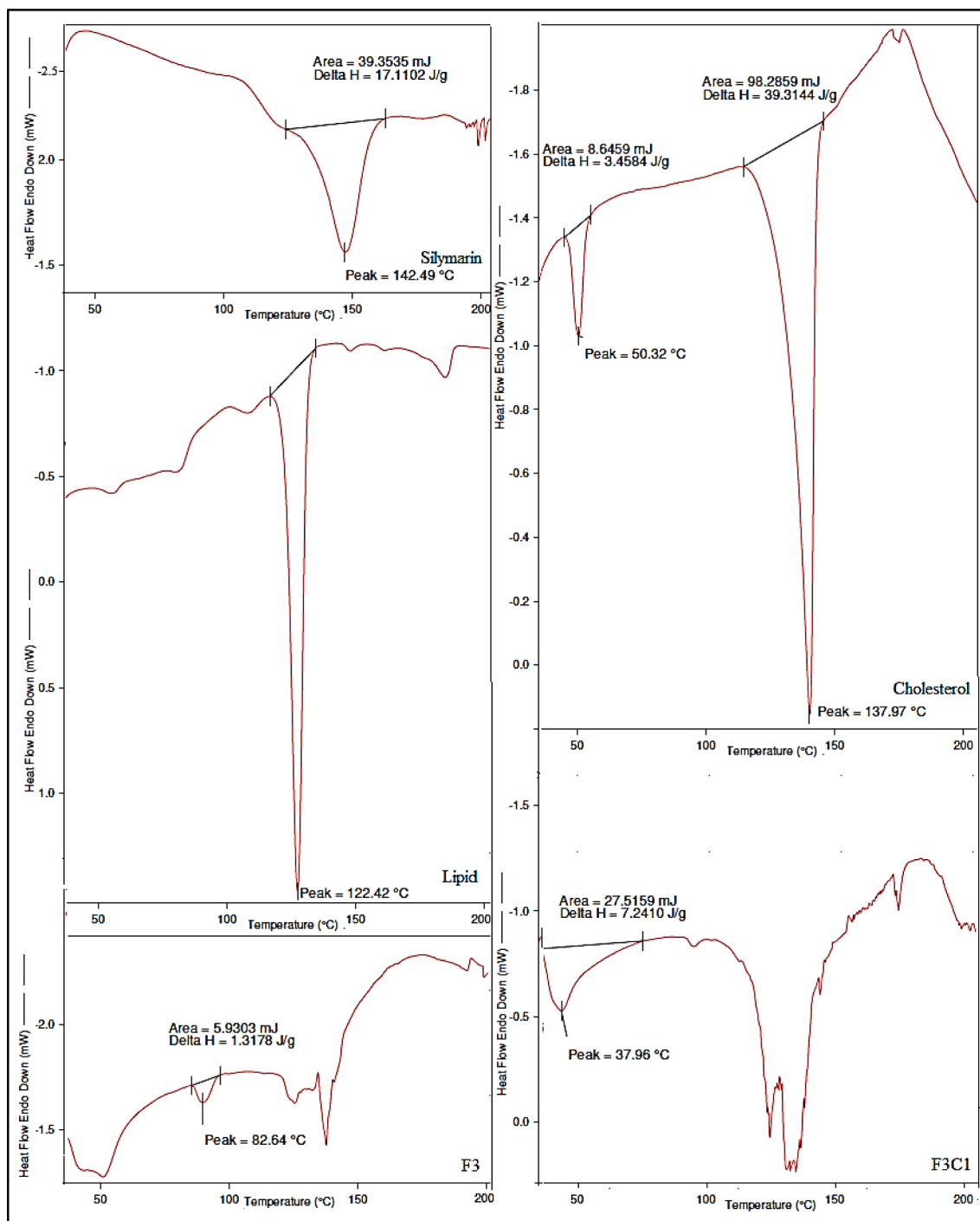
Fig. 4. DSC thermogram of free Silymarin, Lipid, Cholesterol, Silymarin vesicles (F3) and Silymarin surface modified vesicles (F3C1).

chitosan, cholesterol, lipid, SLR vesicles (F3) and SLR surface modified vesicles (F3C1). The free SLR is a flavonoid and it showed the stretching frequency for the phenolic hydroxyl functional group at C-5, C-7 & C-20 was found to be at 3400.76 cm^{-1}. The C–H stretching was seen at 2932.87 cm^{-1} and the carbonyl group at position 4 exhibited the stretching frequency at 1629.77 cm^{-1}. The C-O-C group exhibits the stretching frequency at 1458.78 cm^{-1}. The hydroxyl group at C-3 and C-23 exhibit the stretching frequency at 1079.67 cm^{-1}. The carrier chitosan (CHT) exhibits the stretching frequency for CH$_2$-OH and C–H stretching at 3355.30 cm^{-1} and 2863.77 cm^{-1}. The amide II stretching peak was depicted at 1586.31 cm^{-1}. The cholesterol (CHL) exhibits the hydroxyl stretching peaks of the steroid nucleus at 3409.34 cm^{-1}. The

C–H stretching frequency of the hydrocarbon side chain was exhibited at 2934.47 cm^{-1}. The lipid showed carbonyl stretching frequency at 1732.36 cm^{-1}. This CH$_2$ scissoring frequency peak was observed at 1467.76 cm^{-1}. The C-N and C-O-P stretching frequencies were elucidated at 1380.08 and 1061.40 cm^{-1}, respectively. Moving towards the depiction of the frequencies of vesicle F3, we found the merged frequency of the phenolic hydroxyl group of the drug and the hydroxyl group of the cholesterol at 3329.81 cm^{-1}. The C–H stretching frequency of SLR was also found to be merged with cholesterol (stretching vibration of hydrocarbon side chain) at 2941.95 cm^{-1}. The carbonyl stretching vibration peaks were not seen for either the drug or the carrier phosphatidylcholine. The C-O-P peaks of the lipid carrier were observed
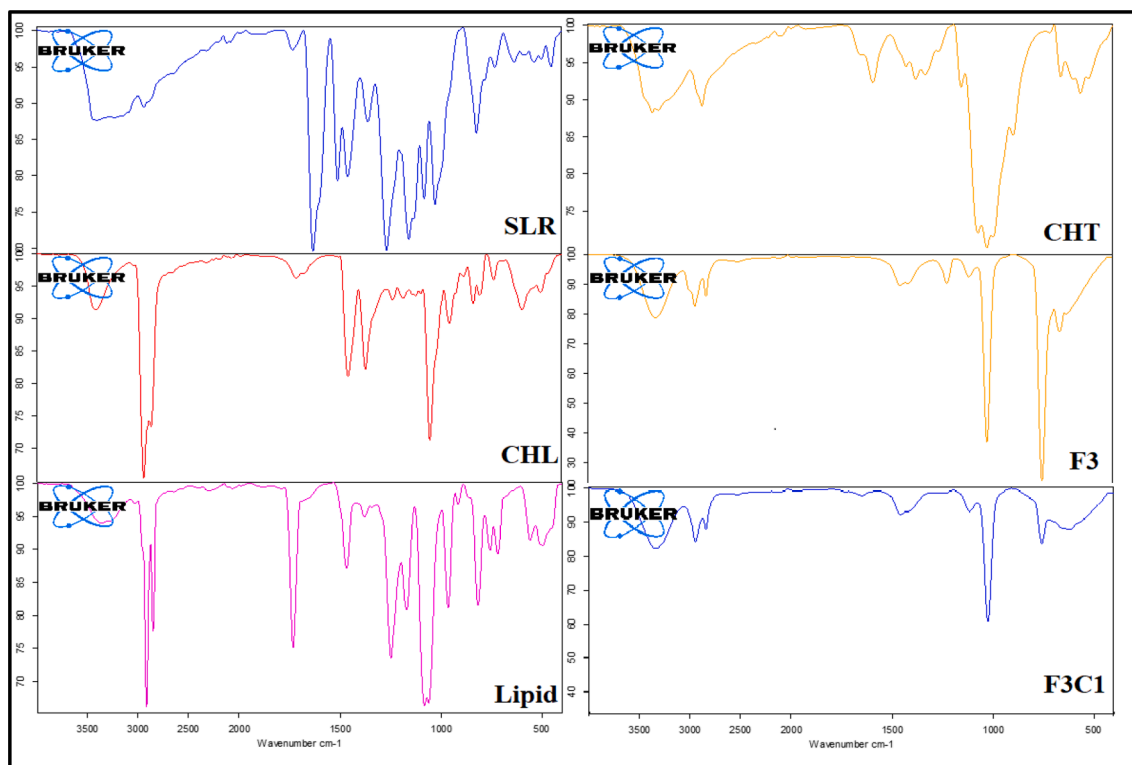
Fig. 5. IR spectra free Silymarin (SLR), Cholesterol (CHL), Lipid, Chitosan (CHT) and Silymarin vesicles (F3) and Silymarin surface modified vesicles (F3C1).

at 1022.78 cm^{-1}. The above observed frequency depicts the formation of vesicles.

The surface modified vesicles (F3C1) exhibits the merged stretching frequency of the free SLR phenolic hydroxyl group and hydroxyl group of the carrier's CHL and CHT, respectively. Similar to the F3, the merged C–H stretching frequency for the SLR and CHL was observed at 2938.16 cm^{-1}. The carbonyl peaks were observed in F3C1 at 1645.48 cm^{-1} for the free SLR and the lipid. The CH$_2$ scissoring peak of the lipid was not observed in F3 and F3C1. There was a drastic change in the peaks of lipid for the C-O-P which was observed at 1020.97 cm^{-1} for F3 and F3C1. The peaks of the amide II group of the CHT were missing in F3C1. The above findings of the frequencies in F3 and F3C1 indicates the formation of SLR vesicles.

3.6. Permeation study

A comparative study was completed for the formulations (F3 and F3C1) and the data compared with the free SLR. All the three samples demonstrated a significant difference in the permeation profile. The free SLR showed the permeation flux of 69.7 ± 3.5 µg/cm^2/h. The optimized formulation (F3) demonstrated a significant ($p < 0.01$) enhancement in the permeation flux (195.1 ± 3.7 µg/cm^2/h) of SLR after formulation into the lipid vesicle. The presence of surfactant enhances the solubility of SLR into the lipid which can easily penetrate across the membrane (Khalifa and Abdul, 2017). In case of the F3C1, the flux was found to be significantly higher than the free SLR dispersion and SLR vesicle (F3). It showed the permeation flux of 291.1 ± 7.7 µg/cm^2/h at the same time. From the results, it was concluded that the SLR lipid vesicles (F3) showed 2.7-folds higher permeation than the free SLR dispersion. But in case of formulation (F3C1) depicted 4.2-folds and 1.5-folds enhancement in the permeation flux than the free SLR and lipid vesicle (F3).

3.7. Antimicrobial study

The results of F3C1 and free SLR showed higher activity against

S. aureus and *M. luteus* (Gram-positive cocci) and *B. pumilus* (Gram-positive rods) bacterial strains (Fig. 6). On the other hand, *E. coli* (Gram-negative rods) showed higher sensitivity to the samples than *B. subtilis* (Gram-positive rods). *P. aeruginosa* strain (Gram-negative rods) showed the least antimicrobial activity among the tested strains. The sample F3C1 showed a significantly higher ($p < 0.05$) or closer to the free SLR against the different bacterial standard strains. The SLR vesicles (F3C1) showed ZOI against *S. aureus* (46 ± 2.9 mm), *B. subtilis* (24 ± 1.8 mm), *M. luteus* (43 ± 3.3 mm), *E. coli* (28 ± 2.7 mm), *P. aeruginosa* (13 ± 2.3 mm), and *B. pumilus* (41 ± 3.8 mm). In case of Free SLR, ZOI was found to significantly lower than SLR vesicles (F3C1) against *S. aureus* (43 ± 4.2 mm, $p < 0.05$), *B. subtilis* (20 ± 2.8 mm, $p < 0.05$), *M. luteus* (38 ± 5.1 mm, $p < 0.05$), and *B. pumilus* (37 ± 3.4 mm, $p < 0.05$). A non-significant difference was found against *E. coli* (29 ± 3.2 mm, ns), and *P. aeruginosa* (13 ± 1.4 mm, ns). The standard drug (Imipenem) depicted ZOI significantly higher against *B. subtilis* (34 ± 2.6 mm, $p < 0.001$), *P. aeruginosa* (28 ± 2.7 mm, $p < 0.001$), lower against *S. aureus* (39 ± 3.5 mm, $p < 0.05$) and *M. luteus* (30 ± 3.9 mm, $p < 0.05$). A non-significant variation was observed against *E. coli* (28 ± 2.5 mm, ns), and *B. pumilus* (40 ± 3.2 mm, ns).

3.8. Antioxidant study

The antioxidant activity was performed for optimized formulation F3C1 and their result compared with the findings of free SLR. Both the samples depicted concentration dependent activity. As the concentration of SLR increases the activity is also enhanced (Fig. 7). In the case of DPPH study, at maximum concentration the free SLR and F3C1 displayed the 94.3 ± 4.3 % and 86.25 ± 2.3 %, respectively. At initial concentration (5, 10, 15 µg/mL), a non-significant variation in the DPPH activity was observed between the free SLR and F3C1. At higher concentration 25 and 50 µg/mL, the variation was found to be significant ($p < 0.05$). A highly significant ($p < 0.01$) difference was observed at the maximum tested concentration 100 µg/mL. A slight different activity was observed in case of ABTS activity. At initial low concentration (5
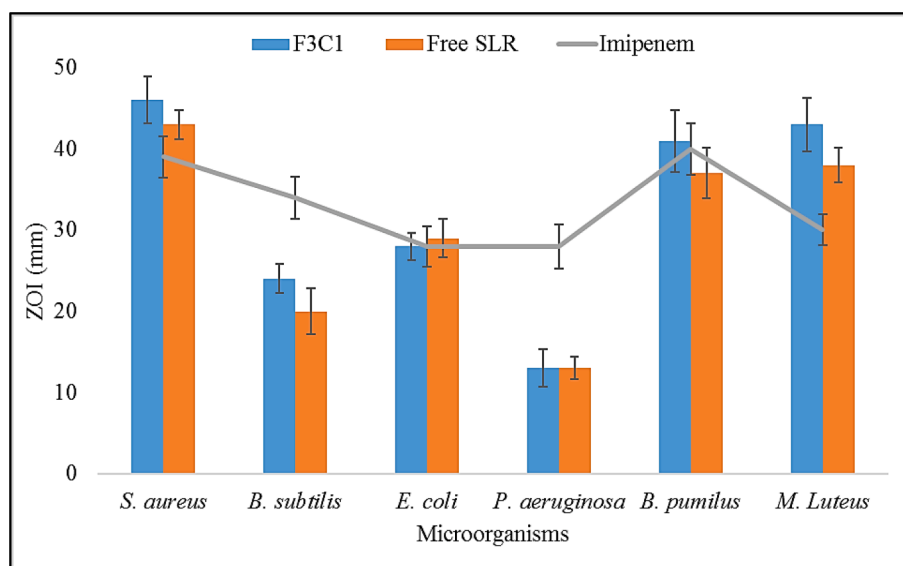
Fig. 6. Antimicrobial activity of free silymarin, silymarin surface modified vesicles (F3C1) and standard drug (Imipenem). Experiment was carried out in duplicate and the mean value was calculated.
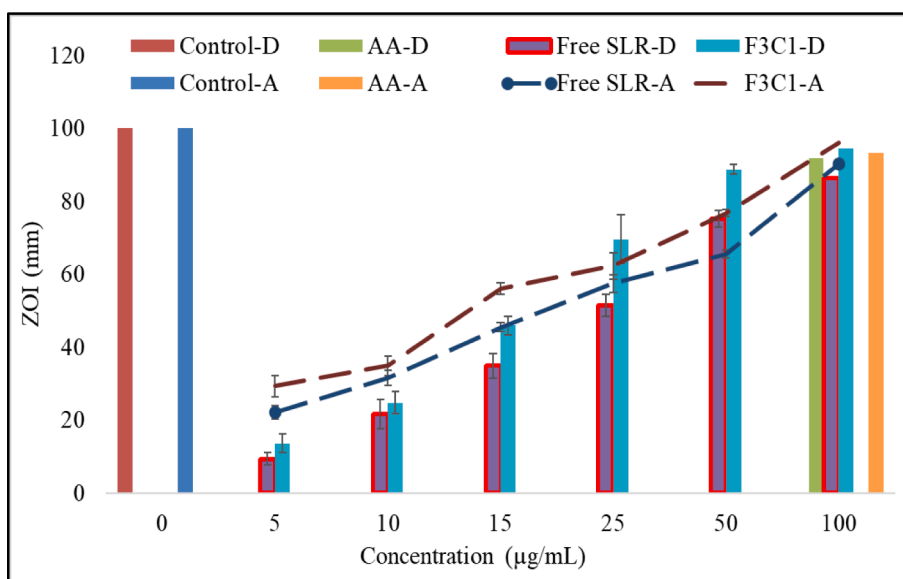

Fig. 7. Antioxidant activity (D-DPPH and A-ABTS) of free silymarin, silymarin surface modified vesicles (F3C1) and standard drug (ascorbic acid). Triplicated data shown as mean ± SD.

and 10 μg/mL), a non-significant difference in the activity was observed. At 15, 25 and 50 μg/mL, a significant ($p < 0.05$) difference in the activity was observed. But at the highest tested concentration (100 μg/mL), the difference was found to be non-significant.

3.9. Cell line study

The assay was performed against lung cancer cell line (HepG2) after treatment with different concentration of free SLR, F3 and F3C1 (Fig. 8). The treated groups were calculated for IC_{50} (drug concentration needed to reduce viability of cells to 50 %). A significant ($p < 0.01$) difference in the IC_{50} was observed for silymarin vesicles F3 and F3C1 was found to be 53.3 μg/mL and 42.6 μg/mL than free SLR (88.6 μg/mL). The low IC_{50} of F3 and F3C1 was found due to the increased solubility of SLR in the used carrier system. The results displayed a concentration dependent activity (Ramakrishnan et al., 2009). At initial concentration (1, 5, 10 μg/mL)

the effect was found to be similar and difference was found to be non-significant. At 25 μg/mL concentration, the cell viability (%) was found to be as follows F3 (68.9, $p < 0.01$) > F3C1 (74.9 %) > free SLR (78.9 %). The higher activity from the vesicle (F3) due the high solubility of SLR at the site than the surface modified vesicles (F3C1). After that a significantly ($p < 0.001$) higher effect was found at concentration (50, 75, 100 μg/mL) for both the samples (F3 and F3C1) than the free SLR. The vesicles (F3) showed 49.3 % (50 μg/mL), 39.6 % (75 μg/mL), 32.7 % (100 μg/mL), whereas surface modified vesicle (F3C1) displayed 39.2 % (50 μg/mL, $p < 0.01$), 30.6 % (75 μg/mL, $p < 0.01$), 21.5 % (100 μg/mL, $p < 0.001$). The free SLR showed lower cell viability at 67.5 % (50 μg/mL), 54.8 % (75 μg/mL), 42.9 % (100 μg/mL). At a concentration of 100 μg/mL, the activity was found 1.3-folds (F3) and 1.9 folds (F3C1) higher than the free SLR.
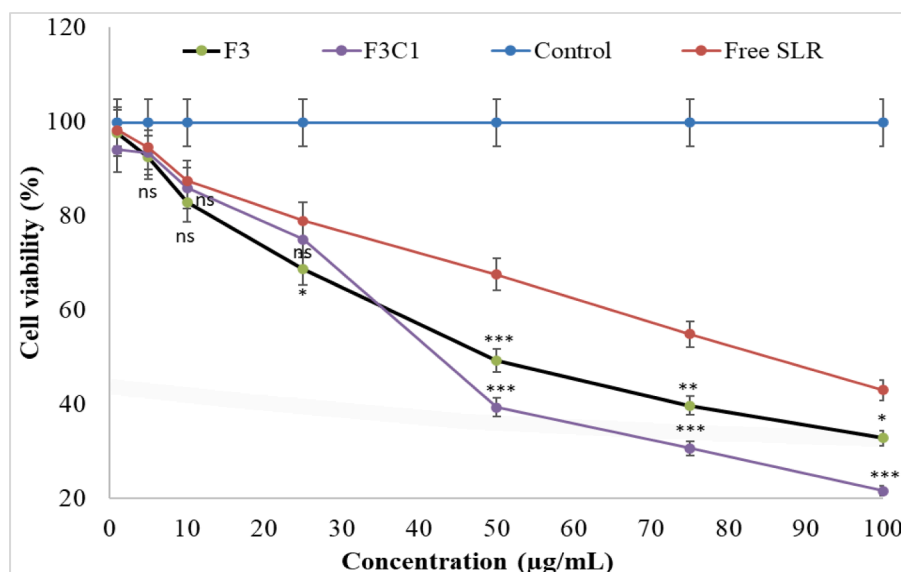
Fig. 8. Cell viability assay of free silymarin, silymarin vesicles (F3) and silymarin surface modified vesicles (F3C1). Triplicated data shown as mean ± SD. Asterisk sign represents the difference in the treatment groups. $p < 0.01$ value statistically significant compared to the free SLR.
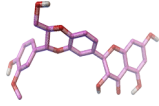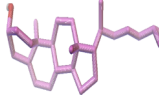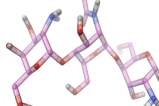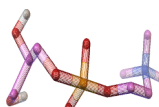
3.10. Molecular docking

The results of the molecular docking of the ligand (SLR & carriers) against VEGFR-2 (3V2A-chain A) was shown in Table 2 **and** Fig. 9**(A-D).** The lowest binding affinity score provides the information about the stability of various docked conformation. The pure SLR exhibited the docking score of −5.42 (Kcal/mol) and formed two hydrogen bonds with the receptor. The distance of one hydrogen bond was found to be 1.994 Å showing the binding interaction of the hydroxyl moiety of phenyl ring in the ligand SLR with the amino acid Arg 23 of the receptor (Fig. 9A). The second hydrogen bond was formed between hydroxyl moiety of the chromene ring of ligand with the amino acid Leu 66 of the receptor having bond length of 1.879 Å. The carrier cholesterol exhibited a binding score of −4.63 Kcal/mol forming one hydrogen bond with the receptor (Fig. 9B). The polar hydrophilic hydroxyl moiety of the hydrophobic steroid skeleton forms a hydrogen bond with the amino acid Asp 63 of the receptor exhibiting bond length of 1.905 Å. The

chitosan **showed a binding** score of −1.15 Kcal/mol forming three hydrogen bonds with the receptor (Fig. 9C). The three-amine moiety of the ligand carrier chitosan forms one hydrogen bond with amino acid ASN 62 having bond length of 2.049 Å and two hydrogen bonds with amino acid GLU 64 having bond length of 2.224 and 2.168 Å, respectively. The lipid exhibits the binding score of −3.58 Kcal/mol. The lipid oxygen moiety of the phosphate group forms 2 hydrogen bonds with the receptor at amino acid CYS 61 and CYS 68 having bond length 2.057 Å and 1.856 Å (Fig. 9D). The other two hydrogen bonds was formed by the oxygen moiety of the lipid fatty acid with the amino acid GLY 59 of the receptor possessing bond length of 1.997 and 1.965 Å, separately.

The drug silymarin is formed from three isomer flavonolignans viz., silybin, silydianin and silychristin. Silybin is proved to be an important and active constituent of silymarin. The study reveals that it inhibits hepatotoxin binding to receptor sites on the membrane of the liver cells, directing to augmented hepatic cells regeneration (Ahmad et al., 2018). The best docked conformation of the ligand and carriers with the

Table 2
Molecular docking details of VEGFR-2 (3V2A-chain A).

| Samples	Structure	Free binding energy (Kcal/mol)	No. of H-bond	Distance of H-bond (Å)	Amino acid residue (Receptor)	Structural features (Ligand)
Silymarin		−5.42	2	1.994	Arg 23	Hydroxyl moiety of phenyl ring
				1.879	Leu 66	Hydroxyl moiety of chromene ring
Cholesterol		−4.63	1	1.905	Asp 63	Polar hydroxyl moiety of steroid ring
Chitosan		−1.15	3	2.049	ASN 62	Amine moiety of D-glucose
				2.2242.168	GLU 64	Amine moiety of D-glucose
Phosphatidyl choline		−3.58	4	2.057	CYS 61	Oxygen moiety of phosphate group
				1.9971.965	GLY 59	Oxygen moiety of fatty acid
				1.856	CYS 68	Oxygen moiety of phosphate group
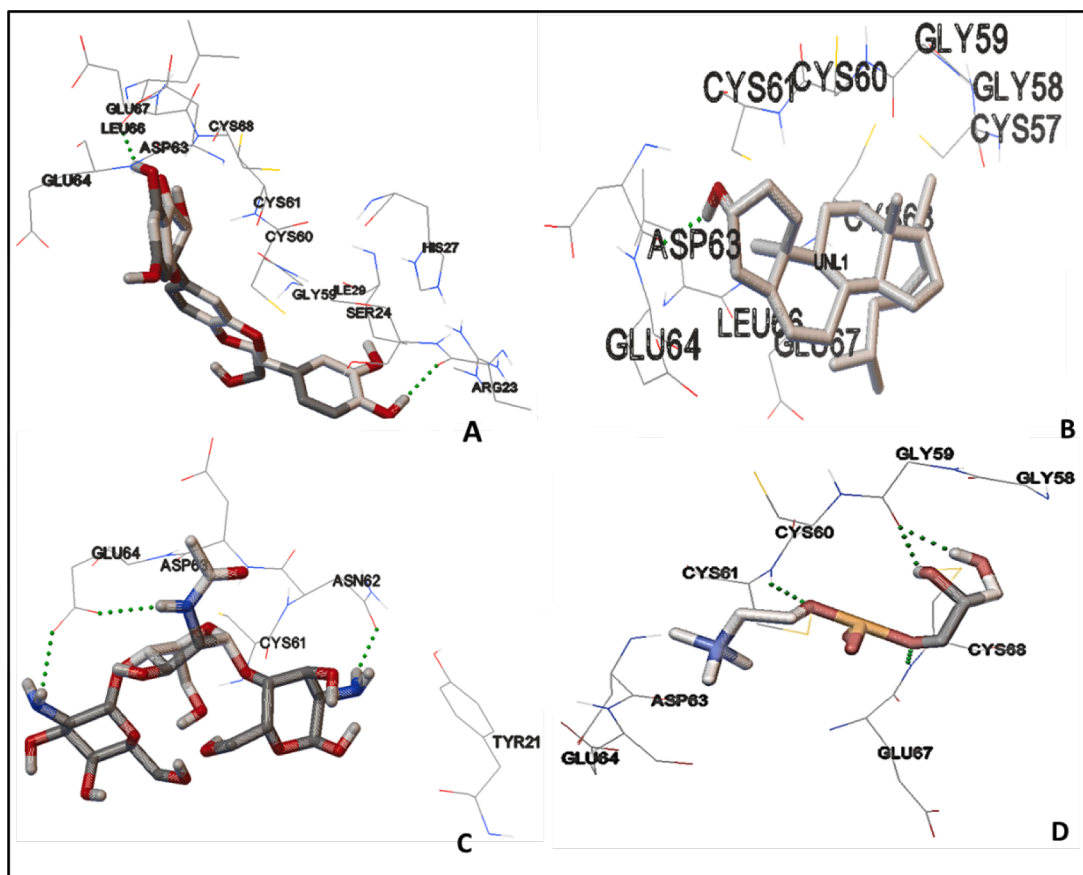
Fig. 9. H-bond interaction of the ligands with receptor. (A: Silymarin, 2H-bond; B: Cholesterol; 1-H bond; C. Chitosan 3-H bond; D. Phosphatidylcholine, 4-H bond.

VEGFR-2 receptor represents the stability of the formed liposomes (Fig. 10). It was presumed from the molecular docking study that the drug and the carriers exhibited anticancer activity against hepatic (Hep G2) cells.

4. Discussion

The low size of the vesicles significantly affects the systemic circulation and cellular internalization. The variation in the size may be due to change in the composition of vesicles. The addition of the chitosan leads to enhanced particle size. The electrostatic repulsion between the similarly charged particles in a dispersion is indicated by the Zeta potential value (Midekessa et al., 2020). A high surface charge will give greater stability for particles because the solution won't tend to agglomerate. It is evident that colloidal solutions with high value (positive or negative) are electrically stable, but low values tend to coagulate or flocculate (Pauna et al., 2023). The addition of chitosan to the lipid vesicles helps to convert surface charge to positive. It also helps to get greater stability than the negatively charged vesicles. The vesicles prepared with phosphatidylcholine, and then further coating them with CHT increased the cationic charge (Hilitanu et al., 2024). The increase in the surfactant concentration leads to significant ($p < 0.01$) enhancement
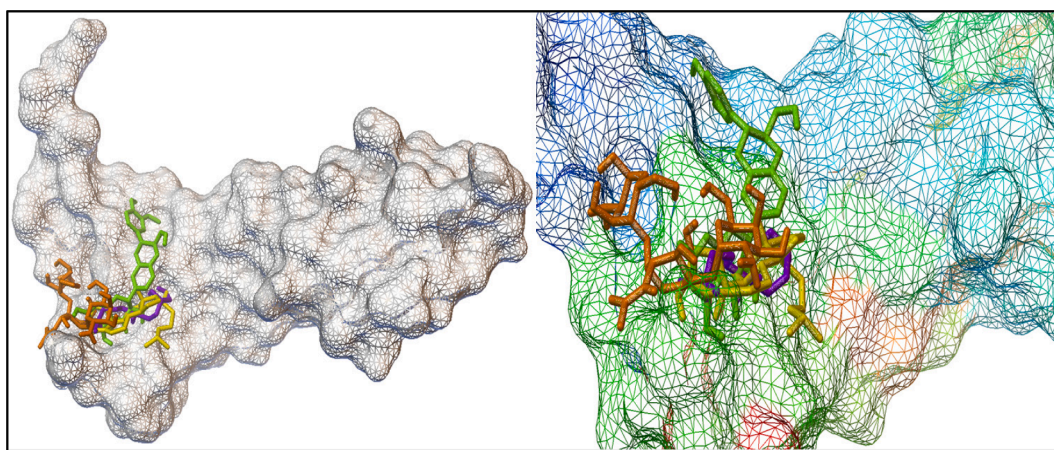

Fig. 10. Docking of Silymarin, Cholesterol, Chitosan and Phosphatidylcholine (Full and zoom view) with VEGFR-2 (PDB ID: 3V2A–chain A) of human hepatocellular carcinoma (HepG2) cells. Silymarin: green colour, Cholesterol: orange colour, Chitosan: purple colour, Phosphatidylcholine: yellow colour.

in the SLR entrapment inside the lipid membrane. It helps to solubilize the maximum amount of SLR by reducing the interfacial tension between the lipid and hydration media. A gradual decrease in the SLR entrapment was observed when the ratio of CHL and PC ratio changes. The reduction in cholesterol concentration changes the SLR entrapment inside the vesicles. The nano size of the vesicles helps to achieve higher drug release because it gets greater effective surface area (Herdiana et al., 2022; Lin et al., 2023).

The release pattern was found to be biphasic, an initial quicker release then a gradual slow release pattern was found. The vesicle (F3) showed about 35 % release in the first 2 h then slow SLR release was found for 12 h. The initial quicker release was found due to the availability of drug on the surface of the vesicle which quickly reaches to the release medium. Later prolonged drug release was found due to the slow diffusion of drug takes place from vesicles and then reaches to the release media from the membrane (Khan et al., 2021). The chitosan formed an extra layer on the vesicles which helped to slow the release of SLR. The slower drug release is ideal for the oral formulation because it helps to achieve maximum drug absorption. The absence of characteristic peaks of SLR in the formulation confirms the conversion of crystalline SLR into amorphous form. The drug completely solubilized in the used carrier so the drug peak was completely absent in the formulation. The low permeation of free SLR may be due to the poor aqueous solubility, which retards the permeation across the membrane. Due to its poor solubility the maximum drug concentration is not available at the membrane surface for the permeation. The presence of surfactant enhances the solubility of the drug into the lipid which can easily penetrate across the membrane (Khalifa and Abdul, 2017). The nano size vesicle also gets greater effective surface area for the drug permeation. The highly significant effect was achieved from F3C1 due to the presence of chitosan in the lipid vesicles. The chitosan helps to enhance the mucoadhesive property and open the tight junction of the membrane. The cationic charge binds with the anionic charge of the membrane, which helps the enhanced permeation of drug (Casettari and Illum, 2014). From the ZOI data, we can say that the used excipients in the formulation does interfere with the antimicrobial property of the SLR. Its activity is significantly higher against the *S. aureus,* and *M. luteus* microorganisms. But against the remaining microorganisms its activities were found to be lesser than the standard drug. The presence of chitosan in the vesicles promotes the antibacterial activities. Chitosan binds to the anionic bacterial cell wall causing damage to the cell. It alters the membrane permeability and inhibition of DNA replication and subsequently cell death (Nagy et al., 1833). The presence of excipients does not interfere with the drug antioxidant activity. It is easily interacting with the DPPH and ABTS solution to depict antioxidant activities. The nano-metric size also helps to achieve better therapeutic activity (Zhang et al., 2004). The higher effective surface area for the solubility leads to a greater amount of drug accumulation at the tumor site (Jinno et al., 2002; Qi et al., 2005). In case of surface modified vesicle (F3C1), the presence of chitosan on the surface lead to cationic surface charge and has a significant impact on their cytotoxic activity. The high cytotoxic effects have been shown by polymers with high cationic charge than by those with low surface charge densities (Fischer et al., 2003). The cationic charged chitosan amino groups and the tumor negative charge electrostatically interact with each other and then harms the cell membrane and organelles (Lee et al., 2002). Ultimately, the damage of the membrane's structure may cause cell death. With the help of docking, we demonstrated that SLR along with the carriers have significantly enhanced the stability of the formed vesicles with possible assumption of anti-proliferative effect in HepG2 cells with variable potency. The findings were also supported by low inhibitory constant (Ki) of SLR values. To culminate, the molecular docking study strengthens our findings against the anti-tumour activity of hepatic cancer cells.

5. Conclusion

In the present study, SLR lipid vesicles (F1 – F6) and SLR surface modified lipid vesicles (F3C1, F3C2) were prepared by the solvent evaporation and hydration method. The prepared SLR lipid vesicles depicted nano size, optimum surface charge and high encapsulation efficiency. IR and DSC analysis displayed no physico-chemical interaction between drug and excipients. The permeation flux demonstrated significant enhancement in the amount of drug permeation from F3C1 than the free SLR and SLR vesicles (F3). The antioxidant and cell viability study results showed concentration dependent activity. The antimicrobial activity result showed a significantly higher activity (F3C1) against the different bacterial standard strains. The enhanced activity was achieved due to the nano-metric size, higher effective surface area and the cationic surface charge of vesicles which displayed a significant impact on their activity.

CRediT authorship contribution statement

Syed Sarim Imam: Conceptualization, Methodology, Writing – original draft. **Sultan Owaid Alshammari:** Funding acquisition, Supervision, Methodology, Writing – review & editing. **Sultan Alshehri:** Funding acquisition, Supervision, Writing – review & editing. **Wael A. Mahdi:** Project administration, Supervision, Validation, Visualization. **Mohamed H. Al-Agamy:** Formal analysis, Methodology, Project administration, Resources.

Declaration of competing interest

The authors declare that they have no known competing financial interests or personal relationships that could have appeared to influence the work reported in this paper.

References

Abdullah, A.S., Sayed, I.E.T.E., El-Torgoman, A.M.A., Kalam, A., Wageh, S., Kamel, M.A., 2022. Green synthesis of silymarin-chitosan nanoparticles as a new nano formulation with enhanced anti-fibrotic effects against liver fibrosis. Int. J. Mol. Sci. 23 (10), 5420.

Ahmad, U., Akhtar, J., Singh, S.P., Badruddeen, Ahmad, F.J., Siddiqui, S., Wahajuddin, 2018. Silymarin nanoemulsion against human hepatocellular carcinoma: development and optimization. Artif. Cells Nanomed. Biotechnol. 46 (2), 231–241.

Alomrani, A., Badran, M., Harisa, G.I., Alshehry, M., Alhariri, M., Alshamsan, A., Alkholief, M., 2019. The use of chitosan-coated flexible liposomes as a remarkable carrier to enhance the antitumor efficacy of 5-fluorouracil against colorectal cancer. Saudi. Pharm. J. 27, 603–611.

Ang, S.S., Thoo, Y.Y., Siow, L.F., 2023. Encapsulation of hydrophobic apigenin into small unilamellar liposomes coated with chitosan through ethanol injection and spray drying. Food Bioproc. Tech. 1–16.

Asmaa, E.F., Sohair, R.F., Amel, M.S., Sherif, A.I., Shimaa, A.S., 2023. A nano-Liposomal formulation potentiates antioxidant, anti-inflammatory, and fibrinolytic activities of Allolobophora caliginosa coelomic fluid: formulation and characterization. BMC Biotech. 23, 28.

Bulbake, U., Doppalapudi, S., Kommineni, N., Khan, W., 2017. Liposomal formulations in clinical use: an updated review. Pharmaceutics 9, 12.

Casettari, L., Illum, L., 2014. Chitosan in nasal delivery systems for therapeutic drugs. J. Control. Release 190, 189–200.

Chambers, C.S., Holeckova, V., Petraskova, L., Biedermann, D., Valentová, K., Buchta, M., Kren, V., 2017. The silymarin composition… and why does it matter??? Food Res. Int. 100 (Pt 3), 339–353.

Clichici, S., David, L., Moldovan, B., Baldea, I., Olteanu, D., Filip, M., Nagy, A., Luca, V., Crivii, C., Mircea, P., et al., 2020. Hepatoprotective effects of silymarin coated gold nanoparticles in experimental cholestasis. Mater. Sci. Eng. C 115, 111117.

CLSI. Performance Standards for Antimicrobial Susceptibility Testing. 32nd ed. CLSI supplement M100. Clinical and Laboratory Standards Institute; 940 West Valley Road, Suite 1400, Wayne, Pennsylvania 19087-1898, USA, 2022.

Collado-González, M., Espinosa, Y.G., Goycoolea, F.M., 2019. Interaction between Chitosan and Mucin: Fundamentals and applications. Biomimetics 4, 32.

Confederat, L.G., Tuchilus, C.G., Dragan, M., Sha'at, M., Dragostin, O.M., 2021. Preparation and antimicrobial activity of chitsan and its derivatives: a concise review. Molecules 26, 3694.

Dawoud, M., 2021. Chitosan coated solid lipid nanoparticles as promising carriers for docetaxel. J. Drug Deliv. Sci. Technol. 62, 102409.

De Luca, M., Lucchesi, D., Tuberoso, C.I., Fernàndez-Busquets, X., Vassallo, A., Martelli, G., et al., 2022. Liposomal formulations to improve antioxidant power of myrtle berry extract for potential skin application. Pharmaceutics 14 (5), 910.

El-Far, Y.M., Zakaria, M.M., Gabr, M.M., Gayar, A.M.E., El-Sherbiny, I.M., Eissa, L.A., 2016. A newly developed silymarin nanoformulation as a potential antidiabetic agent in experimental diabetes. Nanomedicine 11, 2581–2602.

El-Samaligy, M.S., Afifi, N.N., Enas, A., 2006. Mahmoud, Evaluation of hybrid liposomes-encapsulated silymarin regarding physical stability and in vivo performance. Int. J. of Pharm. 319 (1–2), 121–129.

El-Shehawy, A.A., Elmetwalli, A., El-Far, A.H., Mosallam, S.A.E., Salama, A.F., Babalghith, A.O., Mahmoud, M.A., Mohany, H., Gaber, M., El-Sewedy, T., 2023. Thymoquinone, piperine and sorafenib combinations attenuate liver and breast cancers progression: epigenetic and molecular docking approaches. BMC Complementary Med. and Ther. 23, 69.

Fallah, M., Davoodvandi, A., Nikmanzar, S., Aghili, S., Mirazimi, S.M.A., Aschner, M., Rashidian, A., Hamblin, M.R., Chamanara, M., Naghsh, N., et al., 2021. Silymarin (Milk Thistle Extract) as a therapeutic agent in gastrointestinal cancer. Biomed. Pharmacother. 142, 112024.

Federico, A., Dallio, M., Loguercio, C., 2017. Silymarin/silybin and chronic liver disease: a marriage of many years. Molecules 22, 191.

Fischer, D., Li, Y., Ahlemeyer, B., Krieglstein, J., Kissel, T., 2003. In vitro cytotoxicity testing of polycations: influence of polymer structure on cell viability and hemolysis. Biomaterials 24, 1121–1131.

Guimaraes, D., Cavaco-Paulo, A., Nogueira, E., 2021. Design of liposomes as drug delivery system for therapeutic applications. Int. J. Pharm. 601, 120571.

Gutierrez-Saucedo, R.A., Gomez-Lopez, J.C., Villanueva-Briseno, A.A., Topete, A., Soltero-Martinez, J.F.A., Mendizabal, E., Jasso-Gastinel, C.F., Taboada, P., Figueroa-Ochoa, E.B., 2023. Pluronic F127 and P104 polymeric micelles as efficient nanocarriers for loading and release of single and dual antineoplastic drugs. Polymers 15, 2249.

Haddad, F., Mohammed, N., Gopalan, R.C., Ayoub, Y.A., Nasim, M.T., Assi, K.H., 2023. Development and optimisation of inhalable EGCG nano-liposomes as a potential treatment for pulmonary arterial hypertension by implementation of the design of experiments approach. Pharmaceutics 15, 539.

Herdiana, Y., Wathoni, N., Shamsuddin, S., Muchtaridi, M., 2022. Drug release study of the chitosan-based nanoparticles. Heliyon 8, e08674.

Hilitanu, L.N., Mititelu-Tartau, L., Popa, E.G., Buca, B.R., Gurzu, I.L., Fotache, P.A., Pelin, A.-M., Pricop, D.A., Pavel, L.L., 2024. Chitosan soft matter vesicles loaded with acetaminophen as promising systems for modified drug release. Molecules 29, 57.

Huang, J., Zhang, X., Tang, Q., Zhang, F., Li, Y., Feng, Z., Zhu, J., 2011. Prognostic significance and potential therapeutic target of VEGFR2 in hepatocellular carcinoma. J. Clin. Pathol. 64, 343–348.

Jinno, H., Ikeda, T., Matsui, A., Kitagawa, Y., Kitajima, M., Fujii, H., Nakamura, K., Kubo, A., 2002. Sentinel lymph node biopsy in breast cancer using technetium-99m tin colloids of different sizes. Biomed. Pharmacother. 56 (Suppl. 1), 213s–s216.

Keshavarz, F., Dorfaki, M., Bardania, H., Khosravani, F., Nazari, P., Ghalamfarsa, G., 2023. Quercetin-loaded liposomes effectively induced apoptosis and decreased the epidermal growth factor receptor expression in colorectal cancer cells: an in vitro study. Iran J Med Sci. 48 (3), 321–328.

Khalifa, A.M., Abdul, R.B.K., 2017. Optimized mucoadhesive coated niosomes as a sustained oral delivery system of famotidine. AAPS PharmSciTech 18 (8), 3064–3075.

Khan, S., Aamir, M.N., Madni, A., Jan, N., Khan, A., Jabar, A., Shah, H., Rahim, M.A., Ali, A., 2021. Lipid poly (ε-caprolactone) hybrid nanoparticles of 5-fluorouracil for sustained release and enhanced anticancer efficacy. Life Sci. 284, 119909.

Koltai, T., Fliegel, L., 2022. Role of silymarin in cancer treatment: facts, hypotheses, and questions. J. Evid. Based Integr. Med. 27, 2515690X211068826.

Kumar, N., Rai, A., Reddy, N.D., Raj, P.V., Jain, P., Deshpande, P., Mathew, G., Kutty, N. G., Udupa, N., Rao, C.M., 2014. Silymarin liposomes improves oral bioavailability of silybin besides targeting hepatocytes, and immune cells. Pharmacol. Rep. 66, 788–798.

Lee, J.K., Lim, H.S., Kim, J.H., 2002. Cytotoxic activity of aminoderivatized cationic chitosan derivatives. Bioorg. Med. Chem. Lett. 12, 2949–2951.

Liang, J., Liu, Y., Liu, J., Li, Z., Fan, Q., Jiang, Z., Yan, F., Wang, Z., Huang, P., Feng, N., 2018. Chitosan-functionalized lipid-polymer hybrid nanoparticles for oral delivery of silymarin and enhanced lipid-lowering effect in NAFLD. J. Nanobiotechnol. 16, 64.

Lin, X., Wang, Q., Du, S., Guan, Y., Qiu, J., Chen, X., Yuan, D., Chen, T., 2023. Nanoparticles for co-delivery of paclitaxel and curcumin to overcome chemoresistance against BC. J. Drug Deliv. Sci. Technol. 79, 104050.

Ma, Y., He, H., Xia, F., Li, Y., Lu, Y., Chen, D., Qi, J., Lu, Y., Zhang, W., Wu, W., 2017. In vivo fate of lipid-silybin conjugate nanoparticles: implications on enhanced oral bioavailability. Nanomedicine 13, 2643–2654.

Machado, A.R., Pinheiro, A.C., Vicente, A.A., Souza-Soares, L.A., Cerqueira, M.A., 2019. Liposomes loaded with phenolic extracts of Spirulina LEB-18: physicochemical characterization and behavior under simulated gastrointestinal conditions. Food Res. Int. 120, 656–667.

Maryam, T., Rana, N.F., Alshahrani, S.M., Batool, F., Fatima, M., Tanweer, T., Alrdahe, S. S., Alanazi, Y.F., Alsharif, I., Alaryani, F.S., et al., 2023. Silymarin encapsulated liposomal formulation: an effective treatment modality against copper toxicity associated liver dysfunction and neurobehavioral abnormalities in Wistar rats. Molecules 28, 1514.

Megahed, M.A., El-sawy, H.S., Reda, A.M., Abd-Allah, F.I., Abu, S.K., Lila, A.E., Ismael, H.R., El-Say, K.M., 2022. Effect of nanovesicular surface-functionalization via chitosan and/or PEGylation on cytotoxicity of tamoxifen in induced-breast cancer model. Life Sci. 307, 120908.

Melchior, S., Codrich, M., Gorassini, A., Mehn, D., Ponti, J., Verardo, G., Tell, G., Calzolai, L., Calligaris, S., 2023. Design and advanced characterization of quercetin-loaded nano-liposomes prepared by high-pressure homogenization. Food Chem. 428, 136680.

Micheli, L., Di Cesare Mannelli, L., Mosti, E., Ghelardini, C., Bilia, A.R., Bergonzi, M.C., 2023. Antinociceptive action of thymoquinone-loaded liposomes in an in vivo model of tendinopathy. Pharmaceutics 15, 1516.

Midekessa, G., Godakumara, K., Ord, J., Viil, J., Lättekivi, F., Dissanayake, K., Kopanchuk, S., Rinken, A., Andronowska, A., Bhattacharjee, S., et al., 2020. Zeta potential of extracellular vesicles: toward understanding the attributes that determine colloidal stability. ACS Omega 5, 16701–16710.

Moya-Garcia, C.R., Li-Jessen, N.Y.K., Tabrizian, M., 2023. Chitosomes loaded with docetaxel as a promising drug delivery system to laryngeal cancer cells: an in vitro cytotoxic study. Int. J. Mol. Sci. 24 (12), :9902.

Nagy, A., Harrison, A., Sabbani, S., Munson, R.S., Dutta Jr., P.K., 1833. Waldman WJ. Int. J. Nanomed. 2011, 6.

Pandey, M., Choudhury, H., Ying, J.N.S., Ling, J.F.S., Ting, J., Ting, J.S.S., Hwen, I.K.Z., Suen, H.W., Kamar, H.S.S., Gorain, B., et al., 2022. Mucoadhesive nanocarriers as a promising strategy to enhance intracellular delivery against oral cavity carcinoma. Pharmaceutics 14, 795.

Parsa, M.B., Tafvizi, F., Chaleshi, V., Ebadi, M., 2023. Preparation, characterization, and Co-delivery of cisplatin and doxorubicin-loaded liposomes to enhance anticancer activities. Heliyon 9, e20657.

Pauna, A.-M.-R., Mititelu Tartau, L., Bogdan, M., Meca, A.-D., Popa, G.E., Pelin, A.M., Drochioi, C.I., Pricop, D.A., Pavel, L.L., 2023. Synthesis, characterization and biocompatibility evaluation of novel chitosan lipid micro-systems for modified release of diclofenac sodium. Biomedicines 11, 453.

Piazzini, V., Rosseti, C., Bigagli, E., Luceri, C., Bilia, A.R., Bergonzi, M.C., 2017. Prediction of permeation and cellular transport of silybum marianum extract formulated in a nanoemulsion by using PAMPA and Caco-2 cell models. Planta Med. 83, 1184–1193.

Piazzini, V., Lemmi, B., D'Ambrosio, M., Cinci, L., Luceri, C., Bilia, A.R., Bergonzi, M.C., 2018. Nanostructured lipid carriers as promising delivery systems for plant extracts: the case of silymarin. Appl. Sci. 8, 1163.

Piazzini, V., D'Ambrosio, M., Luceri, C., Cinci, L., Landucci, E., Bilia, A.R., Bergonzi, M. C., 2019. Formulation of nanomicelles to improve the solubility and the oral absorption of silymarin. Molecules 24 (9), 1688.

Qi, L.F., Xu, Z.R., Li, Y., Jiang, X., Han, X.Y., 2005. In vitro effects of chitosan nanoparticles on proliferation of human gastric carcinoma cell line MGC803 cells. World J. Gastroenterol. 11 (33), 5136–5141.

Ramakrishnan, G., Lo Muzio, L., Elinos-Báez, C.M., Jagan, S., Augustine, T.A., Kamaraj, S., Anandakumar, P., Devaki, T., 2009. Silymarin inhibited proliferation and induced apoptosis in human hepatic cancer cells. Cell Prolif. 42 (2), 229–240.

Sharifi-Rad, J., Quispe, C., Butnariu, M., Rotariu, L.S., Sytar, O., Sestito, S., Rapposelli, S., Akram, M., Iqbal, M., Krishna, A., et al., 2021. Chitosan nanoparticles as a promising tool in nanomedicine with particular emphasis on oncological treatment. Cancer Cell Int. 21, 318.

Singh, E., Osmani, R.A.M., Banerjee, R., Abu Lila, A.S., Moin, A., Almansour, K., Arab, H. H., Alotaibi, H.F., Khafagy, E.S., 2022. Poly"-caprolactone nanoparticles for sustained intra-articular immune modulation in adjuvant-induced arthritis rodent model. Pharmaceutics 14, 519. [.

Soodvilai, S., Tipparos, W., Rangsimawong, W., Patrojanasophon, P., Soodvilai, S., Sajomsang, W., Opanasopit, P., 2019. Effects of silymarin-loaded amphiphilic chitosan polymeric micelles on the renal toxicity and anticancer activity of cisplatin. Pharm. Dev. Technol. https://doi.org/10.1080/10837450.2018.1556690.

Sun, X., Xu, H., Huang, T., Zhang, C., Wu, J., Luo, S., 2020. Simultaneous delivery of anti-miRNA and docetaxel with supramolecular self-assembled "chitosome" for improving chemosensitivity of triple negative breast cancer cells. Drug Deliv. Transl. Res. 11, 192–204.

Suntres, Z., 2011. Liposomal Antioxidants for protection against oxidant-induced damage. J Toxicol. 2011, 152474.

Venugopal, D.C., Senthilnathan, R.D., Maanvizhi, S., Madhavan, Y., Sankarapandian, S., Ramshankar, V., Kalachaveedu, M., 2023. Preparation and characterization of silymarin gel: a novel topical mucoadhesive formulation for potential applicability in oral pathologies. Gels 9 (2), 139.

Yang, G., Zhao, Y., Zhang, Y., Dang, B., Liu, Y., Feng, N., 2015. Enhanced oral bioavailability of silymarin using liposomes containing a bile salt: preparation by supercritical fluid technology and evaluation in vitro and in vivo. Int. J. Nanomed. 10, 6633–6644.

Younis, N., Shaheen, M.A., Abdallah, M.H., 2016. Silymarin-loaded Eudragit® RS100 nanoparticles improved the ability of silymarin to resolve hepatic fibrosis in bile duct ligated rats. Biomed. Pharmacother. 81, 93–103.

Zhang, L., Hu, Y., Jiang, X., Yang, C., Lu, W., Yang, Y.H., 2004. Camptothecin derivative-loaded poly(caprolactone-co-lactide)-b-PEG-b-poly(caprolactone-co-lactide) nanoparticles and their biodistribution in mice. J. Control. Release 96, 135–148.

Zhang, E., Xing, R., Liu, S., Li, K., Qin, Y., Yu, H., Li, P., 2019. Vascular targeted chitosan-derived nanoparticles as docetaxel carriers for gastric cancer therapy. Int. J. Biol. Macromol. 126, 662–672.